Technical University of Denmark

DTU

Interference patterns and extinction ratio of the diatom Coscinodiscus granii

Maibohm, Christian; Friis, Søren Michael Mørk; Ellegaard, M.; Rottwitt, Karsten

DTU Library
Technical Information Center of Denmark

Interference patterns and extinction ratio of the diatom Coscinodiscus *granii*

C. Maibohm,[1,*] **S. M. M. Friis,**[1] **M. Ellegaard,**[2] **and K. Rottwitt**[1]

[1] *Department of Photonics Engineering, Technical University of Denmark, Ørsteds Plads 343, Kgs. Lyngby, 2800, Denmark*

[2] *PLEN, Department of Plant and Environmental Sciences, University of Copenhagen, Thorvaldsensvej 40, 1871 Frederiksberg C, Denmark*

[*]*chmai@fotonik.dtu.dk*

Abstract: We report experimental and theoretical verification of the nature and position of multiple interference points of visible light transmitted through the valve of the centric diatom species Coscinodiscus *granii*. Furthermore, by coupling the transmitted light into an optical fiber and moving the diatom valve between constructive and destructive interference points, an extinction ratio of 20 dB is shown.

References and links

1. O. Pulz and W. Gross, "Valuable products from biotechnology of microalgae," Appl. Microbiol. Biotechnol. **65,** 635–648 (2004).
2. R. Gordon, D. Losic, M. A. Tiffany, S. S. Nagy, and F. A. S. Sterrenburg, "The Glass Menagerie: diatoms for novel applications in nanotechnology," Trends Biotechnol. **27,** 116–127 (2009).
3. W. H. C. F. Kooistra, R. Gersonde, L. K. Medlin, and D. G. Mann, "The origin and evolution of diatoms: their adaption to a planktonic existence," in *Evolution of Primary Producers in the Sea,* P. G. Falkowski and A. H. Knoll, eds. (Elsevier, 2007), pp. 207–250.
4. J. G. Mitchell, L. Seuront, M. J. Doubell, D. Losic, N. H. Voelcker, J. Seymour, and R. Lal, "The role of diatom nanostructures in biasing diffusion to improve uptake in a patchy nutrient environment," PLoS One **8,** e59548 (2013).
5. A. Falciatore and C. Bowler, "Revealing the molecular secrets of marine diatoms," Annu. Rev. Plant Biol. **53,** 109–130 (2002).
6. V. Smetacek, "A watery arms race," Nature **411,** 745 (2001).
7. C. E. Hamm, R. Merkel, O. Springer, P. Jurkojc, C. Maier, K. Prechtel, and V. Smetacek, "Architecture and material properties of diatom shells provide effective mechanical protection," Nature **421,** 841–843 (2003).
8. D. Losic, K. Short, J. G. Mitchell, R. Lal, and N. H. Voelcker, "AFM nanoindentations of diatom biosilica surfaces," Langmuir **23,** 5014–5021 (2007).
9. T. Fuhrmann, S. Landwehr, M. El Rharbl-Kucki, and M. Sumper, "Diatoms as living photonic crystals," Appl. Phys. B Lasers Opt. **78,** 257–260 (2004).
10. K. Kieu, C. Li, Y. Fang, G. Cohoon, O. D. Herrera, M. Hildebrand, K. H. Sandhage, and R. A. Norwood, "Structure-based optical filtering by the silica microshell of the centric marine diatom Coscinodiscus wailesii," Opt. Express **22,** 15992–15999 (2014).
11. S. Yamanaka, R. Yano, H. Usami, N. Hayashida, M. Ohguchi, H. Takeda, and K. Yoshino, "Optical properties of diatom silica frustule with special reference to blue light," J. Appl. Phys. **103,** 074701 (2008).
12. G. Di Caprio, G. Coppola, L. De Stefano, M. De Stefano, A. Antonucci, R. Congestri, and E. De Tommasi, "Shedding light on diatom photonics by means of digital holography," J. Biophotonics **7,** 341–350 (2014).
13. L. De Stefano, I. Rea, I. Rendina, M. De Stefano, and L. Moretti, "Lensless light focusing with the centric marine diatom Coscinodiscus walesii," Opt. Express **15,** 18082–18088 (2007).
14. S.-H. Hsu, C. Paoletti, M. Torres, R. J. Ritchie, A. W. D. Larkum, and C. Grillet, "Light transmission of the marine diatom Coscinodiscus wailesii," Proc. SPIE **8339,** 83390F (2012).
15. E. De Tommasi, I. Rea, V. Mocella, L. Moretti, M. De Stefano, I. Rendina, and L. De Stefano, "Multi-wavelength study of light transmitted through a single marine centric diatom," Opt. Express **18,** 12203–12212 (2010).

16. M. A. Ferrara, P. Dardano, L. De Stefano, I. Rea, G. Coppola, I. Rendina, R. Congestri, A. Antonucci, M. De Stefano, E. De Tommasi, "Optical properties of diatom nanostructured biosilica in Arachnoidiscus sp: Micro-optics from mother nature," PLoS One **9,** 3–10 (2014).
17. E. De Tommasi, I. Rea, L. De Stefano, P. Dardano, G. Di Caprio, M. A. Ferrara, and G. Coppola, "Optics with diatoms: towards efficient, bioinspired photonic devices at the micro-scale," Proc. SPIE **8792,** 87920O (2013).
18. G. R. Hasle and G. A. Fryxell, "Diatoms: cleaning and mounting for light and electron microscopy," Trans. Am. Microsc. Soc. **89,** 469–474 (1970).
19. N. Delen and B. Hooker, "Free-space beam propagation between arbitrarily oriented planes based on full diffraction theory: a fast Fourier transform approach," J. Opt. Soc. Am. A **15,** 857–867 (1998).

1. Introduction

Diatoms are unicellular photosynthetic microorganisms and among the most common phytoplankton in all water environments and have a colossal impact on the primary production of the world contributing with around 25% of the total amount [1,2]. Setting diatoms apart from other phytoplankton is the nanostructured silica shell surrounding the protoplasm, called the frustule, with nanoscale patterning unique for each of the estimated up to 200.000 different species [2,3]. Since diatoms are so widespread and biologically successful although they are not motile, the frustule presumably has some other biological advantage [4–6]. Even though well investigated, the functionality of the frustule is not fully understood but it has been shown that the frustule provides the diatom with several properties; protection from mechanical and biotic stress, efficient nutrition uptake and light harvesting properties [4,7–12]. In this work, focus is on how monochromatic light is transmitted through the valve. When light interacts with the valve the result may be reflection giving rise to iridescence as well as part of the light being coupled to the frustule and subsequently waveguided [9]. Alternatively, light can be transmitted through the valve with diffraction from the foramen (holes) as the important effect. We are interested in developing a simple description of the multiple interference points described in simulations at a distance corresponding to outside the frustule when light interacts with the valve of the centric species Coscinodiscus *granii* (C. *granii*) [10, 12–15]. These interference points have been discussed on a theoretical basis and a few have been showed experimentally [13–17]. To our knowledge, it is the first time that multiple interference points have been shown both experimentally and their positions connected to theoretical prediction. Our experiments have been carried out in air which enhances the refractive index difference and thereby the diffraction effect compared to the natural habitat of diatoms; water (in the case of C. *granii*, saline water). Our findings are compared to simulations which allow us to identify the important structural parameters behind the photonic properties which is necessary to develop applications of the valves in devices or optical components. Furthermore, we show how the interference pattern of the valves can be used as the basis for an optical switch for coupling light into an optical fiber.

2. Materials and methods

2.1. *Diatomic material, sample preparation, and SEM images*

Diatoms of the selected species C. *granii* (strain K-1048 from the Scandinavian Culture Collection of Algae and Protozoa) were grown under cool white light conditions at 15 °C 16/8 h dark/light cycle. The diatoms were harvested and cleaned to remove organic material according to [18]. The individual parts of the frustule were suspended in DI-water after the cleaning process. SEM (Hitachi S-4800) images were made of the valves by drop casting the solution on carbon tape, drying and spotter coating with 2 nm Au-Pd; a typical SEM image of a valve is seen in Fig. 1(a). Valve parameters were extracted from the images and applied in the numerical simulations presented below. Prior to the optical experiments the diatom solution was drop-casted on a microscope slide and dried in ambient air conditions resulting in a dispersed
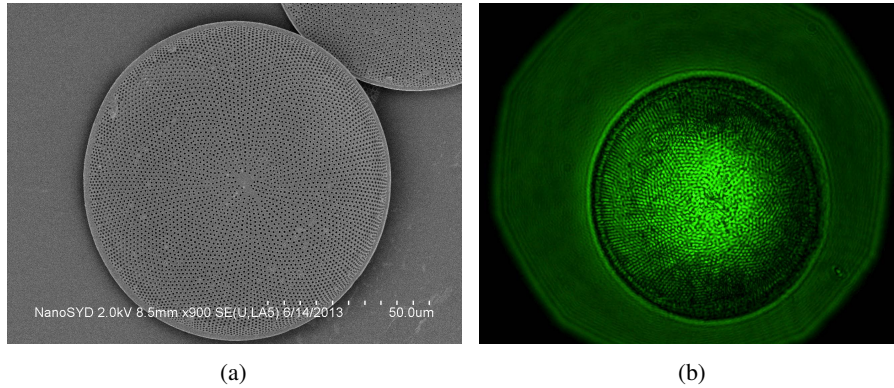
Fig. 1. (a) SEM image of C. *granii*. The pores of the valve are easily seen as well as the non-porous off-centered origin of the structure. (b) High resolution transmission optical image of C. *granii* illuminated by a 532 nm laser, where the light is observed to be primarily transmitted through the holes.

collection of individual valves. A typical image of an individual valve is seen in Fig. 1(b).

2.2. Transmission and extinction ratio measurements

For selection, accurate positioning and movement of the valve on the prepared sample, the microscope slide was mounted on an *x-y-z*-stage that may be moved with sub-micrometer precision. To match the illumination area to the valve size an *x-y*-movable 100 μm pinhole was mounted on the *x-y-z*-stage close to the sample whereby both could be moved in unison. Illumination was either a 632 nm HeNe-laser or a collimated 532 nm diode laser both of which have a Gaussian beam profile before the pinhole. The two laser beams are steered by guiding mirrors and by using a dichroic mirror both laser beams could also illuminate the sample at the same time. A schematic representation of the experimental setup is seen in Fig. 2.

The light transmitted through the diatomic valve was collected by an infinity corrected microscope objective (40× Nikon Plan Fluorite Imaging Objective, 0.75 NA, 0.66 mm WD) and an image plane was created by a tube lens (Thorlabs ITL200 Infinity-Corrected Tube Lens for Plan Fluorite Objectives). Detection at the image plane was done either with a high resolution color CCD camera (Thorlabs DCU224C 1280×1024) or a fiber coupled highly sensitive spectrometer (Ocean optics QEPRO, 0.8 nm resolution). When the CCD camera was used each color (RGB) channel is analyzed independently while size determination was done by imaging a standard target (USAF and Standard Targets, Target Dot Diameter METRIC). For extinction ratio (ER) measurements where a dynamic range intensity range larger than the 2^8 bit of the CCD camera was needed, the spectrometer was mounted as detector. In this configuration the collection end of the 50 μm optical fiber could be moved with micrometer precision in the *x-y*-plane for signal optimization.

2.3. Numerical simulations

Simulations of light propagation through the sample valve is carried out using a Fourier transform approach in which the output field amplitude at distance *z* from the valve is calculated as [19]

$$U(x,y,z=L) = \mathscr{F}^{-1}\left\{\mathscr{F}\left\{U(x,y,z=0)\right\}\exp(ik_zL)\right\} \tag{1}$$
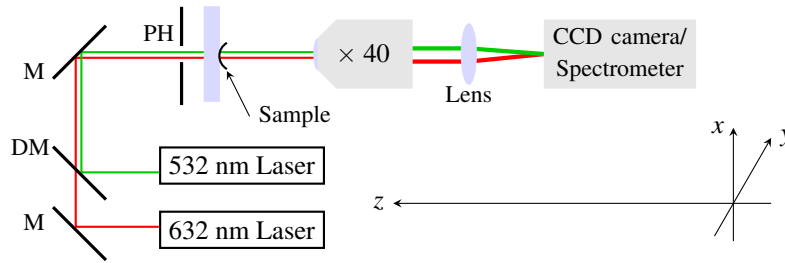
Fig. 2. Experimental setup for transmission and ER experiment. The sample can be illuminated by laser sources at either 632 nm or 532 nm or both at the same time. In the figure; (M) guiding mirrors, (DM) is a dichroic mirror. (PH) is a 100 μm pinhole, 40$\times$ infinity corrected objective with NA $= 0.75$ and a tube lens to create an image plan at the position of the CCD camera or spectrometer.

where $U(x,y,z)$ is the field amplitude at position z as a function of the transverse coordinates x and y, $\mathscr{F}$ denotes the Fourier transform, and $k_z = \sqrt{k_0^2 - k_x^2 - k_y^2}$, where $k_0 = 2\pi/\lambda$ is the wave number. The transverse wave vectors k_x and k_y are calculated for every spatial direction as explained in [19]. The Fourier transform is evaluated using the Fast Fourier Transform algorithm in Matlab. In pursuit of a simple explanation of the multiple interference points, we employ a basic model of a diatom valve: the holes are assumed to be completely transparent and the area between the holes completely opaque, which is a reasonable approximation as seen in Fig. 1(b). The hole pattern in a real valve has two main characteristics: seen from the center, arms are spiraling outwards the edge and new arms are formed when the distance between neighboring arms is large enough. Secondly, looking closely at a limited number of holes, a hexagonal pattern is observed as indicated by the dark green lines in the top picture of Fig. 3(a). This pattern is broken only at places where a new spiraling arm begins. Since a systematic pattern that simulates both these characteristics is difficult to define, we use just a hexagonal pattern as model, which is seen in the bottom picture of Fig. 3(a). The hole diameter, d, and the hole-to-hole distance, Λ, are found to be $d = 0.55$ μm ± 0.1 μm, and $\Lambda = 1.345$ μm ± 0.044 μm from the valve in Fig. 1(a). The valve diameter is found to be approximately 90 μm from the CCD images. The valve model was loaded into Matlab with a resolution of 16 pixels/μm. An electrical field of unit amplitude is then propagated in free space away from the valve and the center $(x = y = 0)$ intensity, where the multiple interference points occur, is saved in every numerical step. To avoid reflections from the boundaries, an absorbing boundary is implemented as well. There are no fitting parameters in the model.

3. Results and discussion

In the transmission experiment, the valve is moved from the focal plan to 215 μm in 1 μm steps along the optical axis where a high resolution CCD image is saved at each step. By stacking the individual images, a cross section out-zooming is created and by extracting the intensity of the center of the valve, a series of constructive and destructive interference points is observed. In Fig. 3(b), plots of the values for the two wavelengths together with results of the simulations are shown: a very good theoretical prediction of the position of the interference points is observed. Hence, we conclude that the multiple interference points stem from diffraction of light coming through the holes of the valve.

For the selected valve with a diameter of 90 μm and illumination at 532 nm, six clearly defined constructive interference points are observed at $z = [127, 136, 148, 163, 178, 197]$ μm, as seen on the top of Fig. 3(b). Seven corresponding destructive interference points are
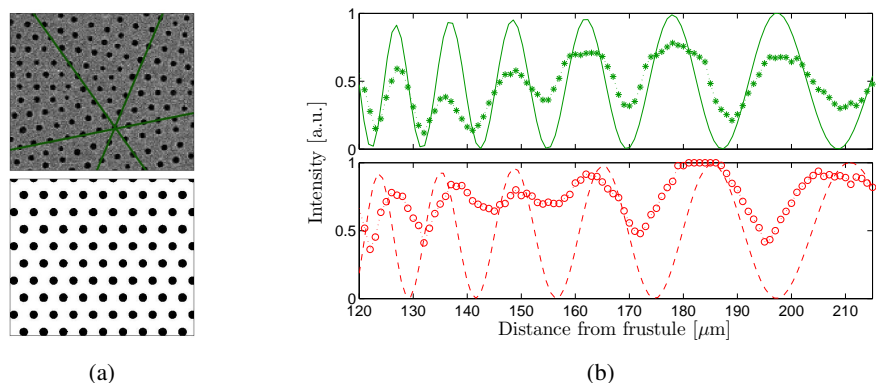
Fig. 3. (a) Top: crop of a SEM image of a valve; the dark green lines indicate the hexagonal structure. The following values are extracted: hole size, 0.548 μm, and hole-to-hole distance 1.345 μm. Bottom: corresponding mask used in the simulations. (b) Transmission experiments at 532 nm (top) and 632 (bottom) where position on the optical axis of the data points (markers) are compared to simulations (solid line). The data points are normalized with 255 (max intensity of the camera) and the simulations are normalized to the maximum value being one.
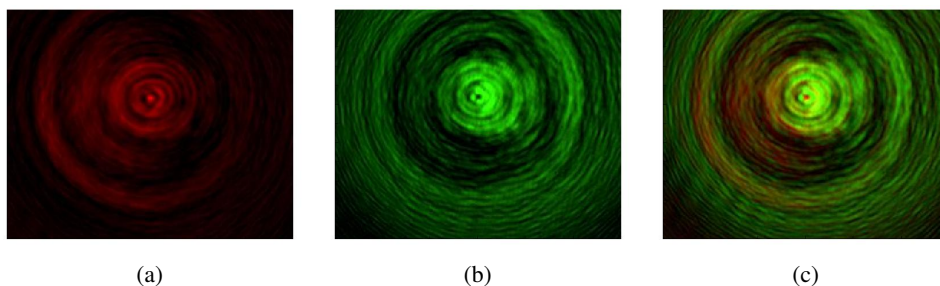

Fig. 4. CCD camera images of the same diatom valve under illumination of: (a) 632 nm, (b) 532 nm, (c) a combination of both. The images are taken at $z = 209$ μm and clearly show a bright center at 632 nm and a dark center at 532 nm.

also identified in the same figure at $z = [123, 132, 141, 155, 170, 189, 208]$ μm. For the same valve and illumination at 632 nm, the six constructive interference points are observed at $z = [127, 138, 149, 161, 183, 207]$ μm. At 632 nm we only clearly identify six destructive interference at $z = [132, 145, 156, 172, 195]$ μm. In Figs. 4(a)–4(c), cross section images at a distance of 207 μm from the focal plane with illumination at 632 nm, 532 nm and where both wavelengths are incident on the valve at the same time are shown. It is clearly seen that the center of the valve is bright, i.e. at a constructive interference point at this distance for illumination at 632 nm and the opposite is the case for illumination at 532 nm.

In the simulations, additional interference points are located at $z < 120$ μm with decreasing period but they cannot be identified in the CCD images due to the limited resolution on the z-axis. It is therefore not possible to absolutely enumerate the individual peaks in the two experiments and identify the shift of position on the optical axis as a function of wavelength. However, since the intensity of the green illumination oscillates faster vs. z than that of the red, we conclude that all interference points are moved closer to the valve with increasing wavelength, which agrees with what one would expect from diffraction theory. The fluctuating
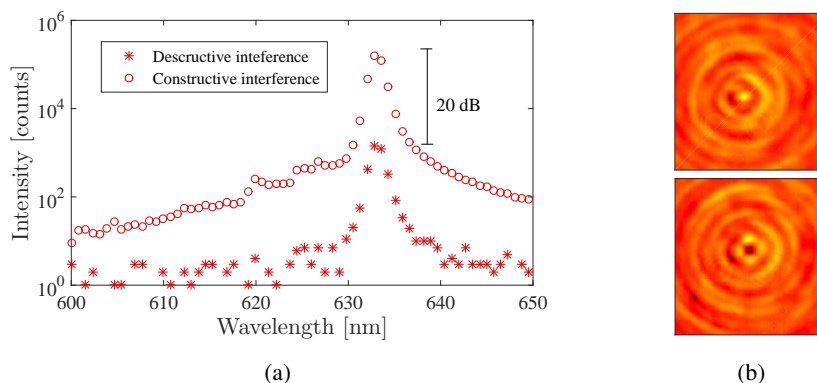
Fig. 5. (a) Spectra for destructive interference (stars) and constructive interference (circles) in the center when the valve is illuminated by 632 nm. The ER is calculated to be 20 dB for the two spectra. (b) Cropped CCD imaged showing the bright center on the top ($z = 207$ μm) and the dark center ($z = 195$ μm) at the bottom used for the extinction experiment.

amplitude of the data points in Fig. 3(b) is caused by imperfections in the valve hole pattern and the partial transparency of the valve, which was assumed opaque in the simulations.

As an example of application, the diatom valve may function as an optical switch for coupling light into an optical fiber. Exploiting its interference properties, the valve is moved 12 μm on the optical axis such that the constructive ($z = 207$ μm) and destructive ($z = 195$ μm) interference points are moved in turn to the fiber end facet. The optical fiber, connected to the spectrometer, has a core diameter of 50 μm and is situated at the center of the image plane. This setup corresponds to collecting light from a circular shape with a diameter of 1.25 μm in the focal plane. The diameter of the bright center in top image in Fig. 5(b) is ~ 6.3 μm in the focal plane while the black center at the bottom in Fig. 5(b) is ~ 4.5 μm; they are both larger than the measuring area of the optical fiber. Signal optimization is done in both cases by moving the optical fiber in the image plane. The ER is calculated as the ratio between intensity in the center when there is constructive and destructive interference. The values are extracted from the spectra seen in Fig. 5(a) and calculated as $\mathrm{ER} = 10\log_{10}\left(P_{\mathrm{bright}}/P_{\mathrm{dark}}\right)$, which gives an ER of ~ 20 dB and an indication that the valves may be used as a basic optical switch.

4. Conclusion

We observed interference points of light passing through a valve of the diatom species Coscinodiscus *granii* that differed in position depending on the wavelength. To confirm the origin of these multiple interference points, we carried out simulations of light propagation through a simple model of a valve and compared the results to our experimental findings. We showed that the simulations with no fitting parameters give predictions of the positions of the interference points that agree very well with our experimental findings. Finally, the ratio of the optical power at the constructive and destructive interference points was found to be approximately 20 dB. These findings may have implication for potential applications, such as optical switches.

Acknowledgment